Heliyon 8 (2022) e12092

Contents lists available at ScienceDirect

Heliyon

journal homepage: www.cell.com/heliyon

Research article

TM9SF1 knockdown decreases inflammation by enhancing autophagy in a mouse model of acute lung injury

Juan Xiao, Xiaofang Shen, Huabo Chen, Lu Ding, Ke Wang, Lihong Zhai *, Chun Mao **

Institute of Neuroscience and Brain Disease, Xiangyang Central Hospital, Affiliated Hospital of Hubei University of Arts and Science, No. 136, Jingzhou Street, Xiangyang, 441000, Hubei, China

ARTICLE INFO

Keywords:
TM9SF1
ALI
Autophagy
Inflammation

ABSTRACT

TM9SF1 is a member of the TM9SF (Transmembrane 9 Superfamily Member) family, which usually has a long N-terminal extracellular region and nine transmembrane domains. TM9SF1's biological function and mechanisms in inflammation are yet unknown. Tm9sf1 was shown to be upregulated in the lung tissues of mice suffering from LPS-induced acute lung injury (ALI). *Tm9sf1* knockout mice were studied, and it was shown that *Tm9sf1* knockout significantly alleviated LPS-induced ALI, as evidenced by higher survival rate, improved pulmonary vascular permeability, decreased inflammatory cell infiltration, and downregulated inflammatory cytokines. TM9SF1 was also demonstrated to be a negative regulator of autophagy in the LPS-induced ALI model *in vitro* and *in vivo*. The autophagy inhibitor 3-MA could counteract the beneficial effects of *Tm9sf1* knockout on ALI. Therefore, we discover for the first time the role and mechanism of TM9SF1 in LPS-induced ALI and establish a relationship between TM9SF1 regulated autophagy and ALI progression, which may provide novel targets for the treatment of ALI.

1. Introduction

Acute lung injury (ALI), an acute inflammatory lung disease with high incidence and mortality, is characterized by a severe inflammatory response, increased alveolar-capillary permeability, and acute respiratory failure [1, 2]. Various factors could induce ALI, such as infection, trauma, and hemorrhagic shock [3]. However, due to the complex and largely unexplored molecular pathogenesis of ALI, no effective therapeutic drugs are currently available in clinical practice [4]. The main therapeutic strategies for ALI are to treat the primary disease while controlling the systemic inflammatory response. Therefore, identifying key molecules and mechanisms that respond to the severe symptoms of ALI and identifying novel effective therapeutic targets is critical.

Autophagy is a biological process that packages invading microbes, damaged organelles, and other cytoplasmic contents into double-membrane vesicles called autophagosomes for degradation [5]. Autophagy has been linked to the progression of ALI, according to research [6, 7]. Lipopolysaccharide (LPS) stimulation could induce autophagy in lung epithelial cells and pulmonary endothelial cells [8]. It is generally believed that autophagy has a protective role in the initiation and development of ALI [9]. When confronted with LPS, Atg4b deficient mice developed more severe lung injury by impairing ATF3 activity [10]. The autophagy inhibitor 3-MA inhibited the pro-autophagy and anti-inflammatory effects of glycyrrhizic acid in LPS-induced ALI [11]. BML-111, a lipoxin A4 receptor agonist, could reduce the levels of proinflammatory cytokines, inhibit apoptosis, and ameliorate LPS-induced ALI by stimulating autophagy [12]. However, some studies found that inhibiting autophagy with 3-MA or Atg5 knockdown ameliorated the symptoms and mortality associated with H5N1 infection [13]. These studies suggest that the protective or harmful roles of autophagy in ALI may be conditional, such as different induced ALI factors or cell types used in the studies.

Transmembrane 9 superfamily proteins (TM9SF) family, also known as nonaspanins, is a member of proteins characterized by a large non-cytoplasmic region and 9 transmembrane domains [14, 15]. In mammals, four members (TM9SF1-4) have been identified [15]. However, the biological functions of the TM9SF family remain unexplored. Only a few studies reported that their expression might be associated with the onset and progression of tumors [16, 17, 18, 19]. Both TM9SF1 and TM9SF4 have been shown to promote autophagy [20, 21]. The functional roles and underlying mechanism of the TM9SF family in inflammation are poorly understood. Tm9sf1-4 were all upregulated in the lung tissues of LPS-induced ALI mice. *Tm9sf1* knockout ($Tm9sf1^{-/-}$) mice had

* Corresponding author.
** Corresponding author.
E-mail addresses: zlh_0302@126.com (L. Zhai), 50001@hbuas.edu.cn (C. Mao).

https://doi.org/10.1016/j.heliyon.2022.e12092
Received 18 January 2022; Received in revised form 6 June 2022; Accepted 25 November 2022
2405-8440/© 2022 The Author(s). Published by Elsevier Ltd. This is an open access article under the CC BY-NC-ND license (http://creativecommons.org/licenses/by-nc-nd/3.0/).

significantly alleviated ALI symptoms, including improved survival rate, decreased pulmonary vascular permeability, alleviative inflammatory cell infiltration, and downregulated inflammatory cytokines. We further found that TM9SF1 negatively regulated autophagy in the LPS-induced ALI model *in vitro* and *in vivo*. The autophagy inhibitor 3-MA was able to remove the protective role of *Tm9sf1* knockout in ALI mice. This study may provide novel targets for ALI treatment.

2. Materials and methods

2.1. Cell lines and ALI cell model

Human lung epithelial adenocarcinoma cells A549 were obtained from the American Type Culture Collection (ATCC) and cultured in DMEM medium (12100-046; Gibco, USA) supplemented with 10% fetal bovine serum (900-108; Gemini, USA). For *in vitro* ALI model, the cells were treated with 10 μg/mL lipopolysaccharide (LPS; L2630, Sigma, USA) for 24 h.

2.2. Animals

Eight-week-old wild-type and *Tm9sf1*$^{-/-}$ C57BL/6 male mice (Shanghai Model Organisms Center, Inc., China) were used to establish the ALI mice model. All experimental procedures and protocols were approved by the Hubei University of Arts and Science Animal Ethics Committee, China. To identify the genotyping, we isolated DNA from the tail of mice and subjected them to PCR using the following primers: m-*Tm9sf1*JCRNA-F 5'-CTTGGCTCAGGAGAAGAGCC-3' and m-*Tm9sf1*JCRNA-R 5'-AGCAGGATGGCGAAGACAAA-3'. RT-PCR was applied to examine the mRNA level of T *Tm9sf1* in *Tm9sf1*$^{-/-}$ and wild-type mice. The primers used were as follows: m-*Tm9sf1*-F 5'-CCTTTGATGCACCTTGTCGC-3' and m-*Tm9sf1*-F 5'-CCCCAGACTGTGGCAAAGAT-3'. m-*Gapdh*-F Primer: 5'-CCTC GTCCCGTAGACAAAATGGT-3'; m-*Gapdh*-R: 5'-TTGAGGTCAATGAAG GGGTCGT-3' served as an internal control.

2.3. ALI mice model

The ALI mice model was established via intraperitoneal (i.p.) injection of 5 mg/kg of LPS (L2630, Sigma) dissolved in PBS. The Wt mice were randomly assigned to 2 groups, while the *Tm9sf1*$^{-/-}$ mice were assigned to 3 groups, with 8 mice in each group. The different groups were treated as follows: (1) Wt-Control: 100 μL of PBS; (2) *Tm9sf1*$^{-/-}$-Control: 100 μL of PBS; (3) Wt-LPS: LPS dissolved in 100 μL of PBS; (4) *Tm9sf1*$^{-/-}$-LPS: LPS dissolved in 100 μL of PBS; (4) *Tm9sf1*$^{-/-}$-LPS+3-MA: 15 mg/kg 3-MA (S1049, Selleck, USA) dissolved in 50 μL of PBS, i.p. injected 1 h before LPS injection (dissolved in 50 μL of PBS) to inhibit autophagy. After LPS treatment for 24 h, the lung tissues and blood were collected for further experiments.

2.4. Histological analysis

The lung tissues were collected at 24 h after ALI induction. The tissues were fixed in 4% formalin overnight, embedded in paraffin, and sliced into 4-μm sections. The tissue sections were stained with hematoxylin and eosin (H&E) and subjected to histopathological evaluation using a light microscope (DSX100, Olympus, Japan). A semiquantitative injury scoring system was employed to evaluate lung injury. The scoring system involved 4 indicators: congestion, edema, inflammation, and hemorrhage [22]. Injury scoring grades ranged from 0 to 4: 0, normal; 1, damage of 0–25%; 2, damage of 25–50%; 3, damage of 50–75%; 4, damage of 75–100%. Four random visual fields were selected for each section.

2.5. Lung W/D weight measurement

The lung tissues were collected at 24 h after ALI induction. The tissues were wiped with a filter paper to remove the blood on the surface, and the wet weight (W) was determined. Then, the lung tissues were incubated at 60 °C for 48 h in an oven, after which the dry weight (D) was determined. Finally, the wet/dry (W/D) ratio was calculated.

2.6. Cell counts and protein quantitation in the bronchoalveolar lavage fluid (BALF)

The mice were anesthetized via i.p. injection with pentobarbitone (50 mg/kg) at 24 h after ALI induction. Then, the bronchoalveolar lavage fluid was analyzed by intratracheal injection with 1 mL of PBS, followed by gentle aspiration, pooling, and re-aspiration. After centrifugation, the cell pellet of the lavage fluid was resuspended in 100 μL of PBS, followed by cell counting. The protein concentration in the supernatant was determined by using a BCA quantitative kit (G2026; Servicebio, China).

2.7. Enzyme-linked immunosorbent assay (ELISA) and MPO activity

The protein levels of Mcp-1 (E4834, Bio Vision, CA), Il-1β (MLB00C Systems, Emeryville, CA), Tnf-α (K1051, Bio Vision) in the serum and lung homogenates were determined by using an ELISA kit. The MPO activity was detected by using an MPO Kit according to the manufacturer's instructions (#A044; Nanjing Jiancheng Bioengineering Institute, China).

2.8. Immunohistochemistry (IHC) assay

The paraffin-embedded tissue sections were incubated at 65 °C for 2 h and then deparaffinized. For IHC staining, the endogenous peroxidase activity was blocked with 3% hydrogen peroxide at room temperature for 15 min. The slides were incubated with a primary antibody anti-Lc3 (12741, Cell Signaling, USA) at 4 °C overnight, followed by washing and incubating with an HRP-conjugated secondary antibody (GB23301, Servicebio) at room temperature for 5 min. The slides were then counterstained with hematoxylin.

2.9. RNA extraction and RT-PCR

Total RNA was extracted by TRIzol (269212, Ambion, USA). First-strand cDNAs were synthesized using the iScript cDNA Synthesis Kit (1708891, BIO-RAD, USA) according to the manufacturer's instructions. The gene primer sequences and the internal controls used are listed in Table 1 qRT-PCR was performed on the ABI7500 system using the iTaq Universal SYBR Green Supermix (1725124, BIO-RAD) under the following conditions: 95 °C for 5 min; 40 cycles at 95 °C for 10 s; and 60

Table 1. RT-PCR primer sequences.

Primer name	Sequence (5'-3')	Organism
GAPDH-F	GGAGCGAGATCCCTCCAAAAT	human
GAPDH-R	GGCTGTTGTCATACTTCTCATGG	human
TNF-α-F	GACAGATGTGGGGTGTGAGAA	human
TNF-α-R	TCTGTGTGCCAGACACCCTA	human
TM9SF1–F	GCACCCTGTCGCACCAAG	human
TM9SF1-R	GACAAAGAAGAGGATGCCGTAC	human
Gapdh-F	ATGACTCTACCCACGGCAAG	mouse
Gapdh-R	TACTCAGCACCAGCATCACC	mouse
Tm9sf1-F	GCCTCTGAAACTGGACACG	mouse
Tm9sf1-R	CCTCTTCCTCCTGGC TCTCT	mouse
Tm9sf 2-F	ACTGTGCTGGTCTCCTTGCT	mouse
Tm9sf 2-R	CAGGGTG CTGGGTTAGGTTA	mouse
Tm9sf 3-F	CTCTGCCTTGGAACATCACA	mouse
Tm9sf 3-R	AGCGTCAGCTTCCTTCACAC	mouse
Tm9sf 4-F	AGAGCGATACAAGGG TGAGAA	mouse
Tm9sf 4-R	CACTTCAGAGATGGGTGTGG	mouse

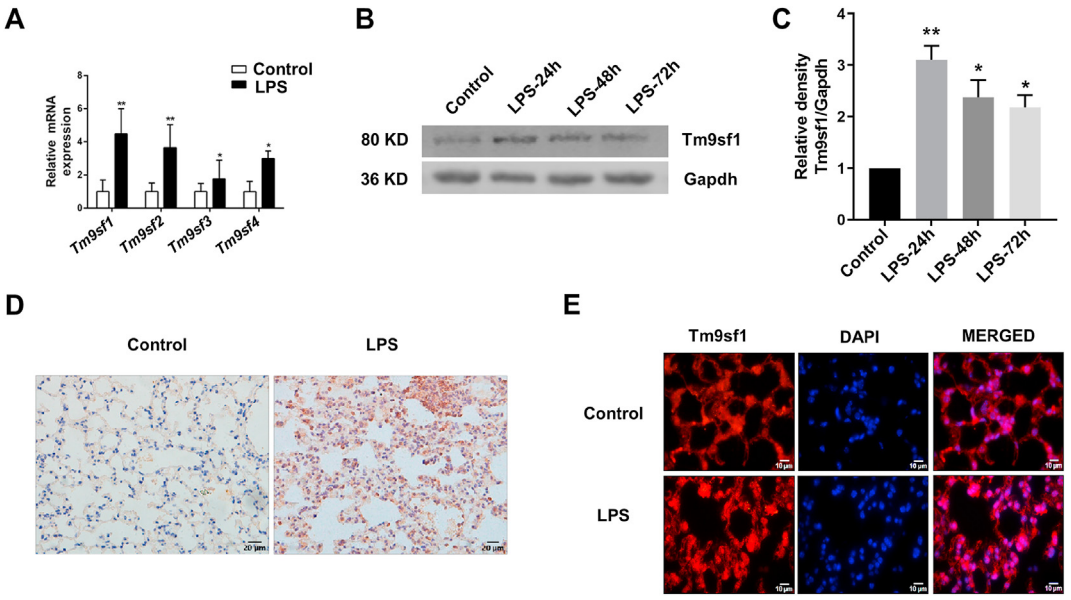

Figure 1. *Tm9sf1* expression in the lung tissues of an ALI mice model. (**A**) The mRNA expression of *Tm9sf1, Tm9sf2, Tm9sf3*, and *Tm9sf4* in the lung tissues of the LPS-induced ALI mice model. The mice were challenged with LPS for 24 h. (**B**) Western blotting analysis of the Tm9sf1 protein levels in the lung tissues of LPS-induced ALI mice model. The mice were challenged with LPS for the indicated time points. (**C**) Quantification of the Tm9sf1 levels relative to that of Gapdh in the lung tissues treated as in (B). (**D-E**) The Tm9sf1 protein levels in the lung tissues of ALI mice were determined by (D) IHC and (E) IF staining. The mice were challenged with LPS for 24 h. *P < 0.05, **P < 0.01. n = 3 in each group.

°C for 20 s. The $2^{-\Delta\Delta Ct}$ method [23] was adopted for the calculation of the relative gene expression. Semi-RT-PCR was also conducted under the following conditions: 95 °C for 5 min; 30 cycles at 95 °C for 20 s; 60 °C for 20 s; 72 °C for 20 s; and 72 °C for 5 min.

2.10. Autophagy flux assays

A549 cells were infected with an adenovirus-expressing tandem mRFP-GFP-LC3 fusion protein (HANBIO, Shanghai, China). After 24 h of

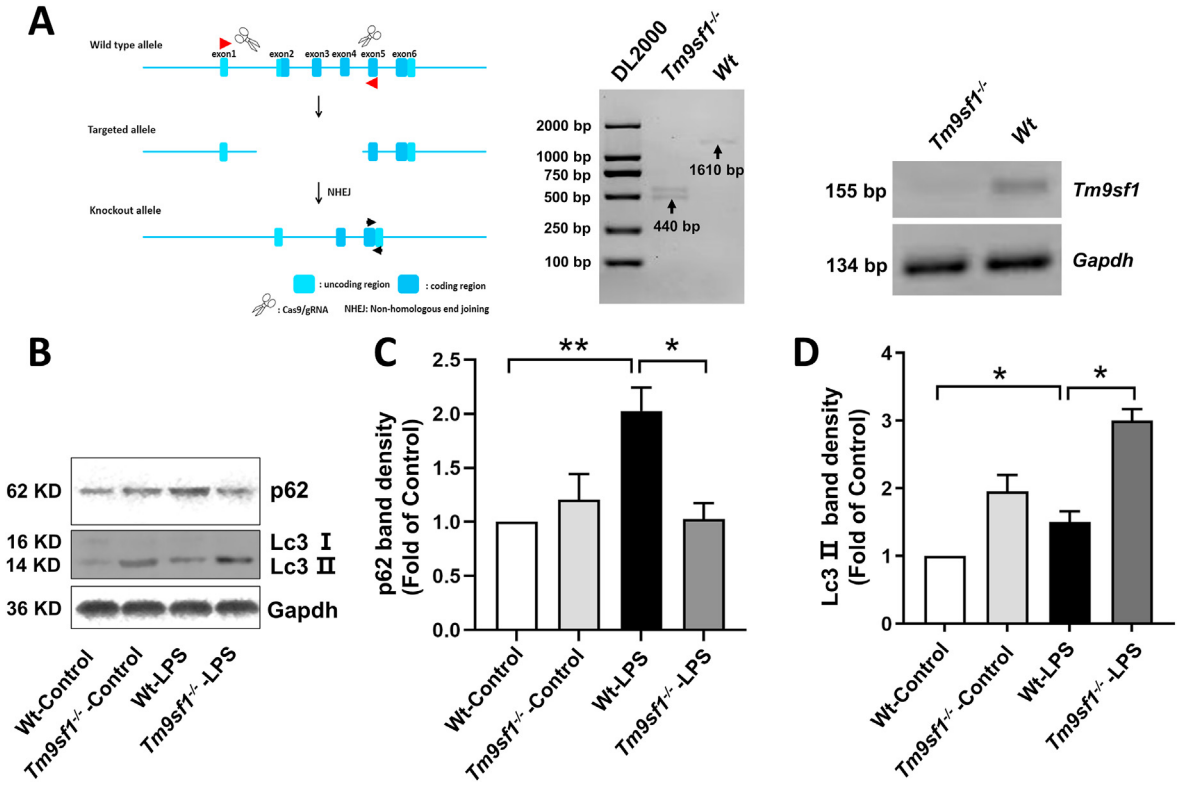

Figure 2. *Tm9sf1* knockout promoted autophagy in the ALI mice model. (**A**) Generation of *Tm9sf1*$^{-/-}$ mice. The left side depicts the *Tm9sf1*-knockout strategy by CRISPR/Cas9. The middle side: Genomic DNA was extracted and analyzed by PCR. The mRNA levels of *Tm9sf1* in *Tm9sf* $1^{-/-}$ and Wt mice are depicted on the right side. (**B**) Western blotting of Lc3-II and p62 protein levels in the lung tissues from Wt-Control, *Tm9sf* $1^{-/-}$-Control, Wt-LPS, and *Tm9sf* $1^{-/-}$-LPS mice. (**C-D**) Densitometric analysis of Lc3-II and p62 bands relative to that of Gapdh in (B). *P < 0.05, **P < 0.01. n = 3 in each group.

infection, the cells were transfected with si-*TM9SF1* or si-Scramble (si-*TM9SF1*: 5'-GGUUACGACCUGACGAGUUTT-3'; si-Scramble: 5'-UUCUCCGAACGUGUCACGUTT-3' (Gene Pharma Company, Suzhou, China) for 24 h. Then, the cells were incubated with 10 ug/mL of LPS for 24 h and fixed with 4% paraformaldehyde. The microphotographs of RFP-GFP-LC3 fluorescence were acquired with a confocal laser scanning microscope (Leica SP8, Germany). Autophagic flux was assessed by counting the number of yellow dots and red dots in each cell (20 cells were scored/each group).

2.11. Western blotting

The western blotting assay was performed as described previously [24]. The primary antibodies used were as follows: anti-Gapdh (AB-P-R 001, GoodHere, China), anti-Tm9sf1 (PA5-84406, Invitrogen, USA), anti-p62 (A7758, ABclonal, China), and anti-Lc3 (12741, Cell Signalling, USA).

2.12. Statistical analysis

Statistical analysis was conducted using the IBM SPSS Statistics 25.0. The student's *t*-test was applied to compare the means between the two groups. One-way analysis of variance (ANOVA) and two-way ANOVA were used for comparison between more than two groups. Unless otherwise mentioned, the values were expressed as means ±SDs. Kaplan–Meier survival analysis was applied to evaluate the survival rate in different groups. $P < 0.05$ was considered to indicate statistical significance. The sample size was calculated using the PASS software by power analysis (1-β = 0.80). GraphPad Prism9 software was conducted for Graph drawing.

3. Results

3.1. Tm9sf1 is upregulated in the lung tissues of ALI mice

We utilized LPS to induce ALI models in mice to evaluate the expression of *TM9SF* members (*TM9SF1-4*). *Tm9sf1* was the most significantly up-regulated member among these four members in the lung tissues of ALI mice (Figure 1A). The protein levels of Tm9sf1 were significantly increased, especially when the mice with LPS were exposed for 24 h (Figures. 1B-C). IHC and IF staining verified the increased Tm9sf1 protein expression (Figure. 1D-E). Tm9sf1 may play important role in the development of ALI induced by LPS, according to our findings.

3.2. Tm9sf1 knockout enhanced autophagy in ALI mice model

To explore the functional roles of TM9SF1 in ALI, we used the CRISPR/Cas9 strategy to generate *Tm9sf1* knockout mice (*Tm9sf1*$^{-/-}$) (Figure 2A). RT-PCR showed that Tm9sf1 expression was completely abolished in *Tm9sf1* $^{-/-}$ mice (Figure 2A). The previous study reported that TM9SF1 could promote autophagy in HeLa cells [20]. Since autophagy plays

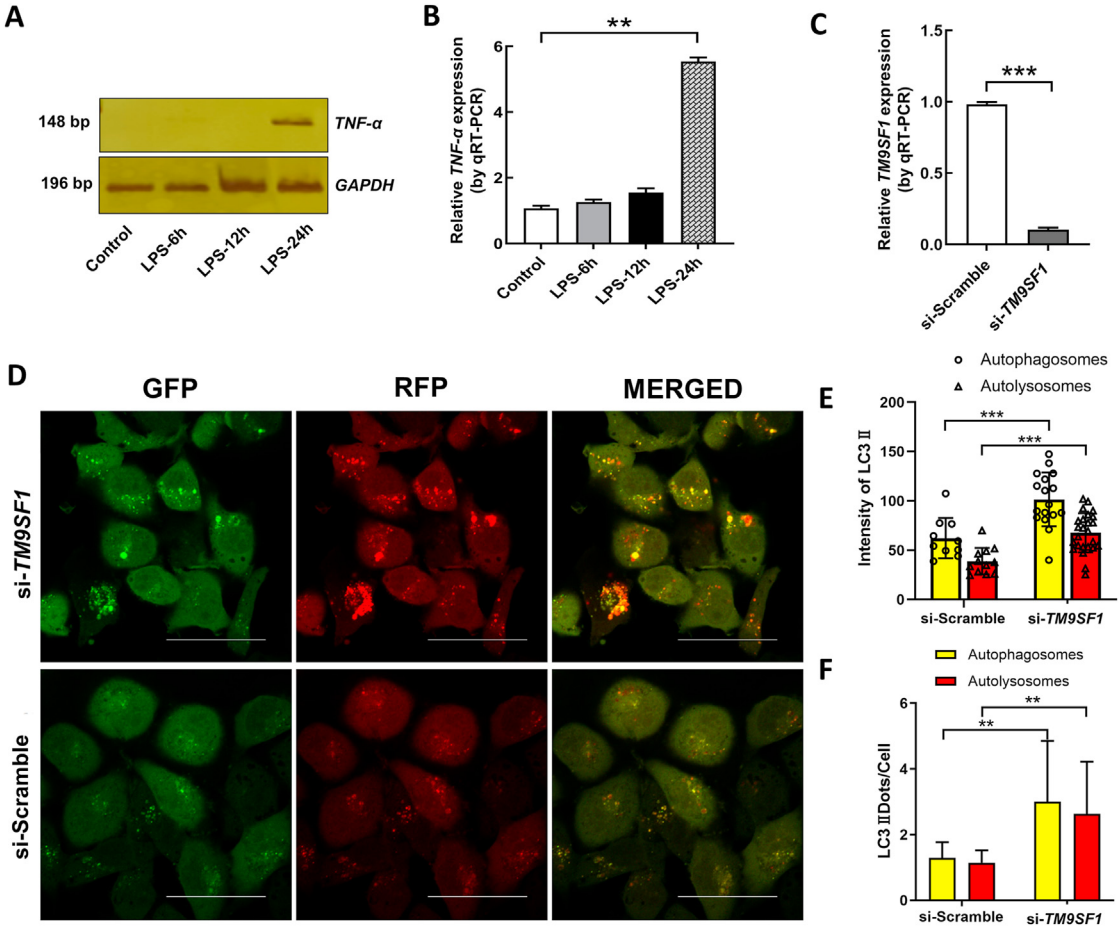

Figure 3. *TM9SF1* knockdown promoted autophagy in A549 cells. (A) Semi-RT-PCR analysis of the *TNF-α* mRNA levels in A549 cells challenged with LPS for the indicated time points. (B) qRT-PCR analysis of the *TNF-α* mRNA levels in A549 cells challenged with LPS for the indicated time points. (C) qRT-PCR analysis of *TM9SF1*-knockdown efficiency in A549 cells transfected with si-*TM9SF*1 or si-Scramble. (D) *TM9SF1*-knockdown A549 cells and control cells were infected with adenovirus-expressing tandem RFP-GFP-LC3 and treated with LPS for 24 h. RFP-GFP-LC3B puncta distribution was observed by confocal microscopy. Representative confocal microscopy images are shown. (E–F) Fluorescence intensity quantitation (E) and dot quantitation of autophagosomes and autolysosomes (F) in cells treated as in (D). Scale bar = 50 μm. *P < 0.05, **P < 0.01. n = 20 cells in each group.

important role in the initiation and development of ALI [25], we wonder whether *Tm9sf1* knockout affects autophagy in the ALI mice model. Surprisingly, the autophagosome marker Lc3-II was up-regulated in the lung tissues of *Tm9sf1*$^{-/-}$ mice compared to control mice. *Tm9sf1* knockout decreased p62, an endogenous autophagy substrate degraded during the autophagic process (Figure 2B-D). These results suggest that *Tm9sf1* knockout enhances autophagy in LPS-induced lung injury.

3.3. TM9SF1 knockdown enhanced autophagy in vitro

We next investigated the regulation of TM9SF1 on autophagy *in vitro*. TNF-α was increased when lung epithelial adenocarcinoma cells A549 were treated with LPS for 24 h, indicating that A549 can be used to establish the *in vitro* model of ALI (Figure 3A-B). We further infected the cells with adenovirus expressing tandem mRFP-GFP-LC3 fusion protein,

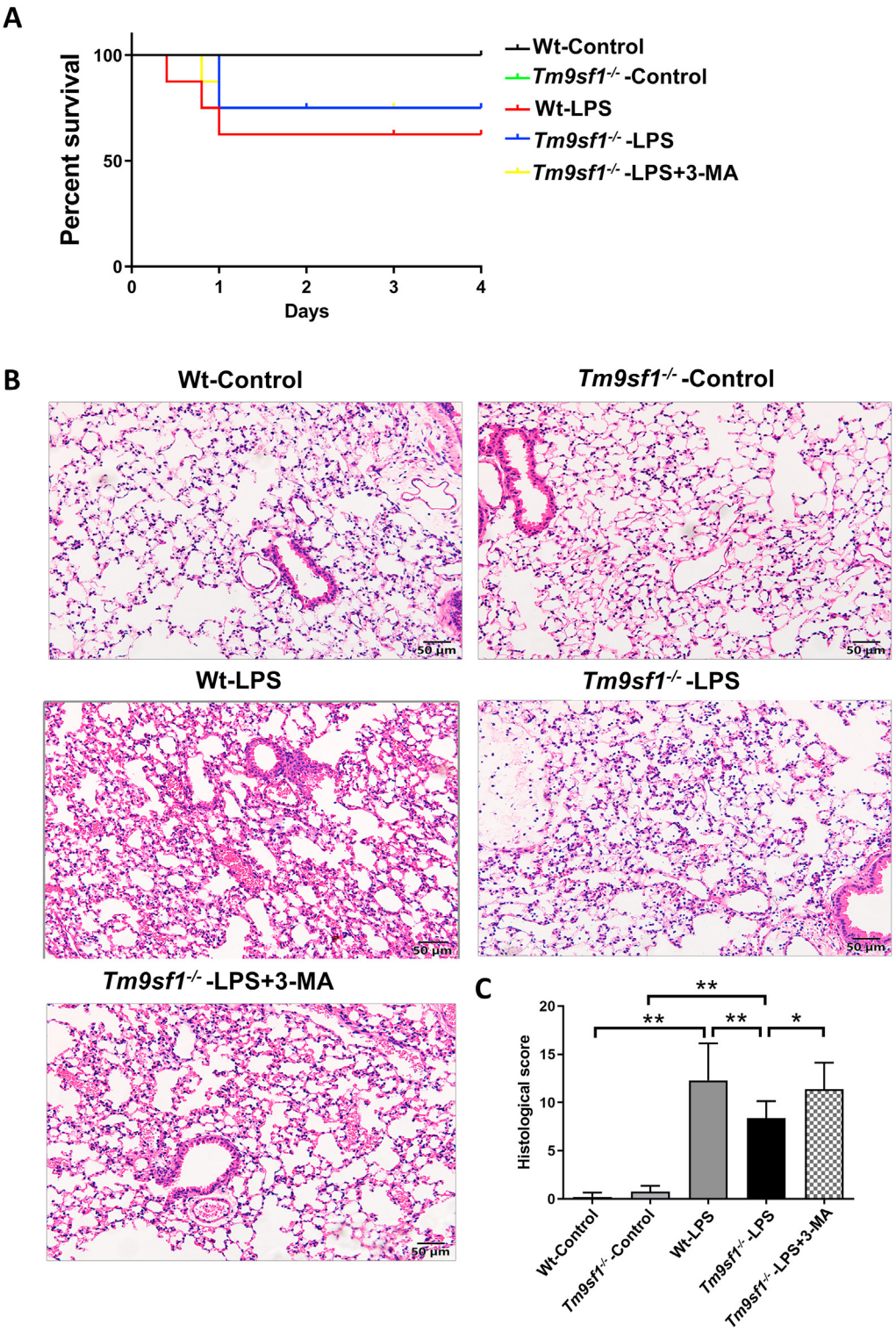

Figure 4. *Tm9sf1* knockout improved the survival rate and ameliorated lung injury in an ALI mice model. Wild type and *Tm9sf1*$^{-/-}$ mice were challenged with LPS or PBS combined with or without 3-MA for 24 h. (A) Kaplan–Meier survival analysis of the mice in different groups. (B) Representative H&E staining of the lung tissues in different groups. (C) The lung injury scores in (B). *P < 0.05, **P < 0.01. n = 8 in each group.

which is used to identify autophagosomes (RFP positive/GFP positive) and autolysosomes (GFP-negative/RFP-positive). GFP fluorescence is quenched in cellular compartments with low pH when autophagosomes fuse with lysosomes [26]. *TM9SF1* knockdown increased the number of autolysosomes and autophagosomes in A549 cells treated with LPS (Figure 3C-F), suggesting that *TM9SF1* knockdown promotes autophagy *in vitro*.

3.4. Tm9sf1 knockout improved lung inflammatory injury in ALI mice depending on autophagy

The effects of *Tm9sf1* knockout on ALI progression were also discovered. The pulmonary epithelium of *Tm9sf1*$^{-/-}$ mice developed normally compared with wild-type mice (Figure 4B). LPS could induce acute lung injuries, such as alveolar collapse, stroma haemorrhagia, pulmonary edema, and inflammatory cell infiltration [8]. These symptoms, however, were alleviated when *Tm9sf1* was knocked out (Figure 4B-C). When confronted with LPS, *Tm9sf1*$^{-/-}$ mice had a higher survival rate (Figure 4A). Then we detected whether Tm9sf1 regulated autophagy was involved in its effect on ALI. 3-MA, an inhibitor for phosphatidylinositol 3-kinases, could abolish the beneficial effects of *Tm9sf1* knockout on ALI (Figure 4A-C). These results demonstrated that *Tm9sf1* knockout improved lung injury in ALI mice depending on autophagy.

3.5. Tm9sf1 knockout decreased pulmonary epithelial barrier permeability and inflammatory cell infiltration in ALI mice

LPS may cause pulmonary edema and increased protein levels in BALF by increasing pulmonary epithelial barrier permeability [27]. In LPS-treated mice, the lung wet/dry ratio and protein concentration in BALF were significantly increased (Figure 5A-B). Myeloperoxidase (MPO), a neutrophil marker, indicates the degree of inflammatory cell infiltration and the progression of lung injury in ALI [28]. In the lung tissues of LPS-treated mice, the total cell count, percentage of neutrophils, and MPO activity were all higher than in wild-type mice (Figures. 5C-E). *Tm9sf1* knockout could attenuate the increased wet/dry ratio, BALF's protein levels, total cell count, percentage of neutrophils, and MPO activity induced by LPS (Figures. 5A-E). Moreover, administration of 3-MA inhibited the protective effects induced by *Tm9sf1* knockout (Figures. 5A-E).

3.6. Tm9sf1 knockout decreased inflammatory cytokine levels in the serum and pulmonary tissues of ALI mice

MCP-1, IL-1β, and TNF-α are inflammatory cytokines that play important roles in the progression of ALI [29]. The levels of Il-1β, Tnf-α, and Mcp-1were evaluated in the serum and lung homogenate of mice from the Wt-Control, *Tm9sf1*$^{-/-}$ Control, Wt-LPS, *Tm9sf1*$^{-/-}$-LPS, and *Tm9sf1*$^{-/-}$-LPS+3-MA groups. The results showed that Il-1β, Tnf-α, and Mcp-1 levels were decreased in the *Tm9sf1*$^{-/-}$-LPS group compared to the Wt-LPS group. 3-MA reversed the anti-inflammatory effects induced by *Tm9sf1* knockout (Figures. 6A-B).

3.7. 3-MA reversed the autophagy enhancement in Tm9sf1 knockout ALI mice

Finally, we analyzed the change of autophagy in the lung tissues from the Wt-Control, *Tm9sf1*$^{-/-}$-Control, Wt-LPS, *Tm9sf1*$^{-/-}$-LPS, and *Tm9sf1*$^{-/-}$-LPS+3-MA groups. Lc3-II protein levels were increased in the *Tm9sf1*$^{-/-}$-LPS group, while p62 protein levels were decreased in the Wt-LPS group. 3-MA could suppress the enhanced autophagy induced by *Tm9sf1*$^{-/-}$ knockout (Fig. 7A-C).

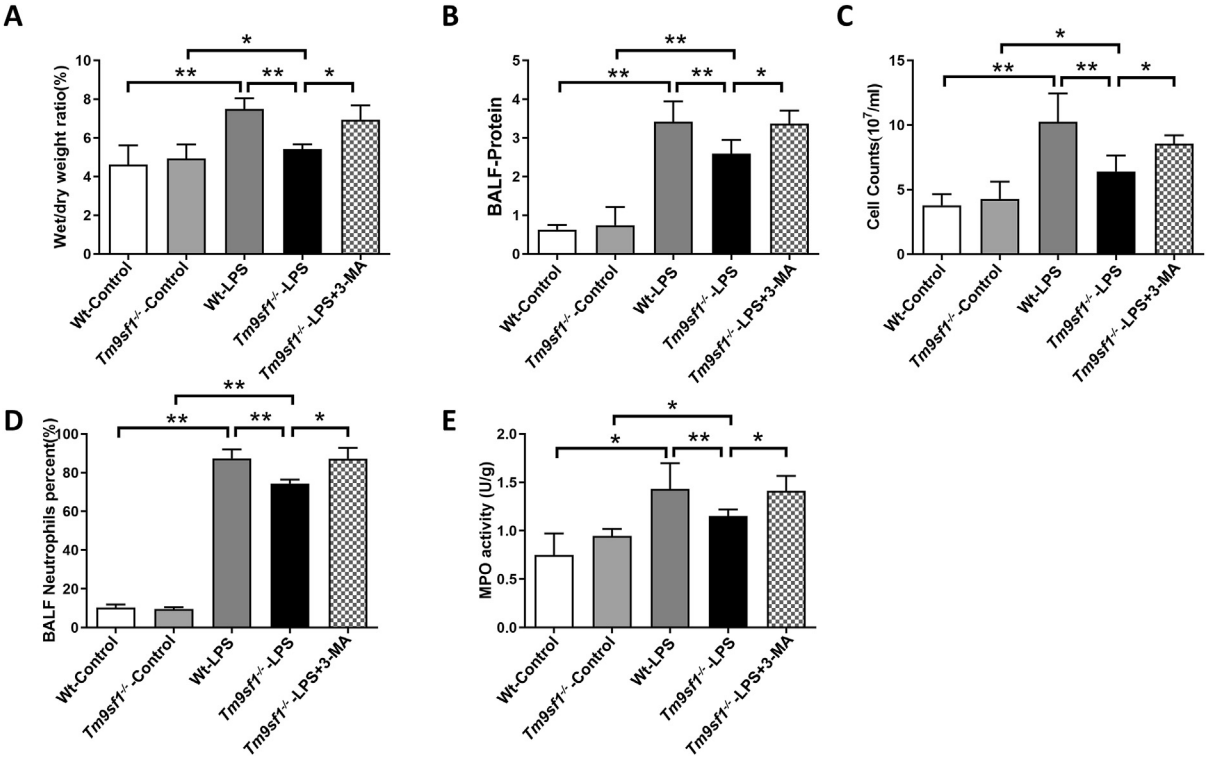

Figure 5. *Tm9sf1* knockout decreased inflammatory cell infiltration in ALI mice. (A) Wet lung/dry lung weight ratio in Wt-Control, *Tm9sf1*$^{-/-}$-Control, Wt-LPS, *Tm9sf1*$^{-/-}$-LPS, and *Tm9sf1*$^{-/-}$-LPS+3-MA groups. (B) Protein concentrations of BALF in Wt-Control, *Tm9sf1*$^{-/-}$-Control, Wt-LPS, *Tm9sf1*$^{-/-}$-LPS, and *Tm9sf1*$^{-/-}$-LPS+3-MA groups. (C) Total cells of BALF in Wt-Control, *Tm9sf1*$^{-/-}$-Control, Wt-LPS, *Tm9sf1*$^{-/-}$-LPS, and *Tm9sf1*$^{-/-}$-LPS+3-MA groups. (D) Neutrophil percentage of BALF in Wt-Control, *Tm9sf1*$^{-/-}$-Control, Wt-LPS, *Tm9sf1*$^{-/-}$-LPS, and *Tm9sf1*$^{-/-}$-LPS+3-MA groups. (E) Myeloperoxidase (MPO) activity in the supernatant of lung homogenate from Wt-Control, *Tm9sf1*$^{-/-}$-Control, Wt-LPS, *Tm9sf1*$^{-/-}$-LPS, and *Tm9sf1*$^{-/-}$-LPS+3-MA groups. *P < 0.05, **P < 0.01. n = 8 in each group.

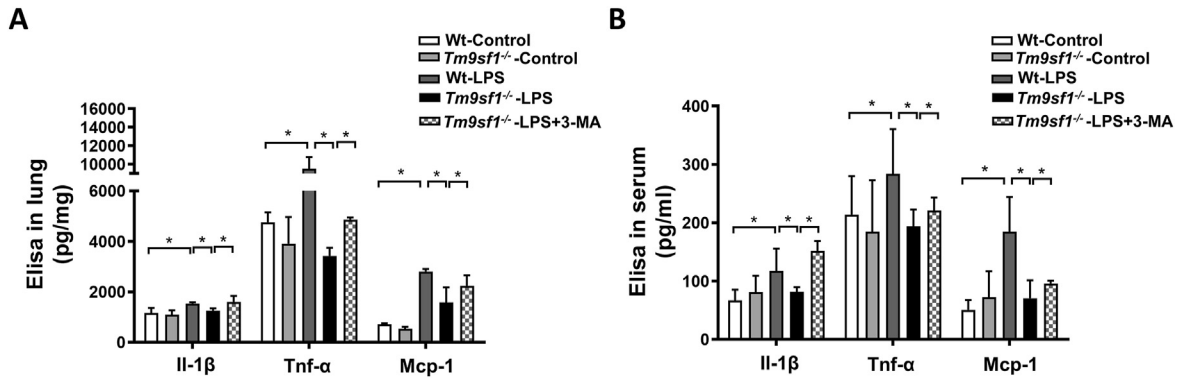

Figure 6. *Tm9sf1* knockout suppressed inflammation in LPS-induced an ALI mice model. (A) Il-1β, Tnf-α, and Mcp-1 levels in the serum from Wt-Control, *Tm9sf1*$^{-/-}$ Control, Wt-LPS, *Tm9sf1*$^{-/-}$-LPS, and *Tm9sf1*$^{-/-}$-LPS+3-MA groups. (B) Il-1β, Tnf-α, and Mcp-1 levels in the supernatant of lung homogenate from Wt-Control, *Tm9sf1*$^{-/-}$ Control, Wt-LPS, *Tm9sf1*$^{-/-}$-LPS, and *Tm9sf1*$^{-/-}$-LPS+3-MA groups. *P < 0.05. n = 8 in each group.

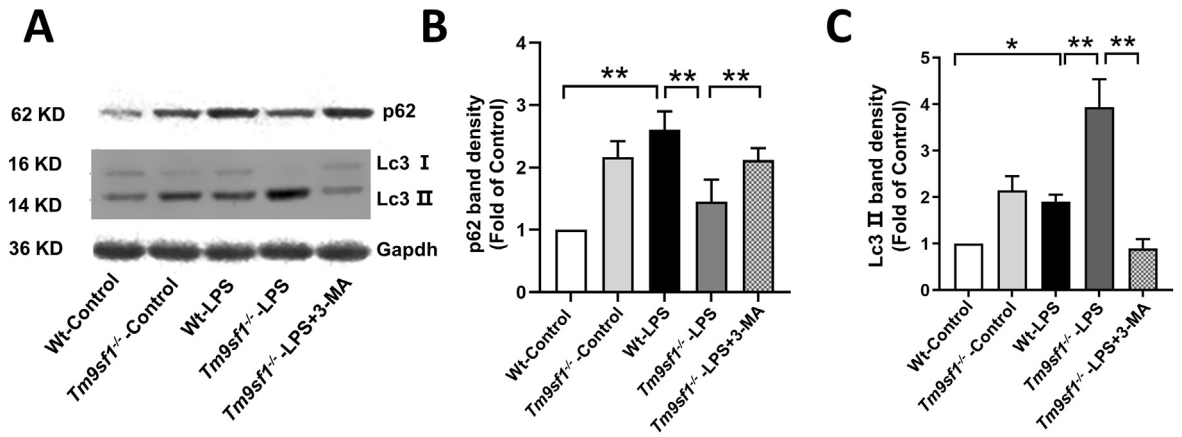

Figure 7. 3-MA inhibited the enhanced autophagy induced by *Tm9sf1* knockout. (A) Lc3-II and p62 protein levels in the lung tissues from Wt-Control, *Tm9sf1*$^{-/-}$-Control, Wt-LPS, *Tm9sf1*$^{-/-}$-LPS, and *Tm9sf1*$^{-/-}$-LPS+3-MA groups. (B, C) Densitometric analysis of Lc3-II and p62 bands in (A). *P < 0.05, **P < 0.01. n = 8 in each group.

4. Discussion

The TM9SF family (TM9SF1-4 in mammals), a class of evolutionarily conserved proteins, are widely expressed in various tissues [30]. The biological function of the TM9SF family is currently unknown. In this study, we found that all four TM9SF members were upregulated in the lung tissues of LPS-induced ALI mice models, suggesting potential roles of the TM9SF family in the progression of inflammatory diseases. We further established *Tm9sf1*$^{-/-}$ knockout mice and found that *Tm9sf1* knockout significantly improved LPS-induced ALI, as evidenced by improved survival rate, decreased pulmonary vascular permeability, inflammatory cell infiltration, and downregulated inflammatory cytokines. Therefore, TM9SF1 may be an unfavorable factor in LPS-induced ALI progression.

ALI progression evolves with a series of genetic and pathway alterations. Autophagy has been shown to play an important role in this process among these mechanisms [31]. A previous study reported that TM9SF1 colocalized with the autophagosome marker LC3 and enhanced autophagy in HeLa cells [20]. TM9SF1 is an autophagy suppressor in LPS-induced ALI, as evidenced by the accumulation of GFP-RFP-LC3 in the TM9SF1 knockdown A549 cells, and the upregulation of LC3-II and decreased p62 protein levels *in Tm9sf1* knockout mice. A possible explanation for these contradictory results might be the two studies' differing cell or tissue contexts. TM9SF1 was also detected in the mitochondria of A549 cells (data not shown), but not in HeLa cells. The molecular mechanism of how TM9SF1 modulates autophagy requires further study.

The relationship between autophagy and ALI is complicated since it has both protective and inhibitory functions. The autophagy inhibitor 3-MA might negate the protective effects of genipin in ALI [32]. 3-MA could also abolish glycyrrhizic acid's pro-autophagy and anti-inflammatory effects on LPS-induced ALI [11]. However, another study reported that the autophagy inhibitor 3-MA protects against endothelial cell barrier dysfunction in LPS-induced ALI [33], and that macrophage-specific *Atg5* knockout mice exhibited attenuated symptoms in Ischemia-reperfusion (IR)-induced ALI [34]. Silencing autophagy-related genes (si*ATG5* or si*ATG7*) or the autophagosome-lysosome fusion inhibitor chloroquine markedly reduced pulmonary microvascular endothelial cell permeability and attenuated LPS-induced ALI [13, 27, 35]. The reason for these different findings is currently unclear. We speculate that targeting different molecules or genes in various types of pulmonary cells may affect autophagy via different molecular mechanisms, thus having distinct roles in the progression of ALI. For example, RAB26 interacted with ATG16L1 and protected endothelial cell permeability, which is dependent on autophagic degradation of phosphorylated SRC [36]. H_2S (hydrogen sulfide) treatment attenuated ventilator-induced ALI by inhibiting autophagy via the ROS/AMPK/mTOR pathway [37]. In brief, our study showed that *Tm9sf1* knockout-induced autophagy protects against LPS-induced ALI. However, the specific mechanism through which *Tm9sf1* knockout improves ALI by regulating autophagy remains unclear and requires additional investigation.

In the present study, we observed that TM9SF1 was upregulated in LPS-exposed mouse lung tissues. *Tm9sf1* knockout could significantly improve LPS-induced ALI. Autophagy may play a crucial role in the development of LPS-induced inflammatory lung injury. TM9SF1 knockout attenuates LPS-induced ALI by activating autophagy. However,

the underlying mechanism by which *Tm9sf1* knockout improves ALI via regulating autophagy remains unclear and needs to be further studied. In summary, the present study suggests that TM9SF1 may be a new therapeutic target for ALI treatment.

Declarations

Author contribution statement

Juan Xiao, Chun Mao: Conceived and designed the experiments; Wrote the paper.

Xiaofang Shen, Huabo Chen: Performed the experiments; Wrote the paper.

Lu Ding: Performed the experiments; Analyzed and interpreted the data; Wrote the paper.

Ke Wang: Analyzed and interpreted the data; Wrote the paper.

Lihong Zhai: Conceived and designed the experiments; Performed the experiments; Wrote the paper.

Funding statement

Juan Xiao was supported by the scientific and technological research projects of Hubei Education Department [D20202602], Subject fund of Hubei University of Arts and Science [2021kptd02].

Data availability statement

Data included in article/supp. material/referenced in article.

Declaration of interest's statement

The authors declare no conflict of interest.

Additional information

No additional information is available for this paper.

Acknowledgements

The authors would like to thank all the reviewers who participated in the review and MJEditor (www.mjeditor.com) for its linguistic assistance during the preparation of this manuscript.

References

[1] R.G. Khemani, et al., Paediatric acute respiratory distress syndrome incidence and epidemiology (PARDIE): an international, observational study, Lancet Respir. Med. 7 (2) (2019) 115–128.
[2] N.T. Mowery, W.T.H. Terzian, A.C. Nelson, Acute lung injury, Curr. Probl. Surg. 57 (5) (2020), 100777.
[3] J. Li, et al., The reaction pathway of miR-30c-5p activates lipopolysaccharide promoting the course of traumatic and hemorrhagic shock acute lung injury, BioMed Res. Int. 2022 (2022), 3330552.
[4] D. Mokra, Acute lung injury - from pathophysiology to treatment, Physiol. Res. 69 (Suppl 3) (2020) S353–S366.
[5] V. Deretic, Autophagy in inflammation, infection, and immunometabolism, Immunity 54 (3) (2021) 437–453.
[6] H. Zhao, et al., Autophagy activation improves lung injury and inflammation in sepsis, Inflammation 42 (2) (2019) 426–439.
[7] S. Vishnupriya, et al., Autophagy markers as mediators of lung injury-implication for therapeutic intervention, Life Sci. 260 (2020), 118308.
[8] D. Zhang, et al., Autophagy maintains the integrity of endothelial barrier in LPS-induced lung injury, J. Cell. Physiol. 233 (1) (2018) 688–698.
[9] L. Qin, et al., Mechanistic target of rapamycin-mediated autophagy is involved in the alleviation of lipopolysaccharide-induced acute lung injury in rats, Int. Immunopharm. 78 (2020), 105790.
[10] A. Aguirre, et al., Defective autophagy impairs ATF3 activity and worsens lung injury during endotoxemia, J. Mol. Med. (Berl.) 92 (6) (2014) 665–676.
[11] L. Qu, et al., Glycyrrhizic acid ameliorates LPS-induced acute lung injury by regulating autophagy through the PI3K/AKT/mTOR pathway, Am. J. Transl. Res. 11 (4) (2019) 2042–2055.
[12] H. Liu, et al., Lipoxin A4 receptor agonist BML-111 induces autophagy in alveolar macrophages and protects from acute lung injury by activating MAPK signaling, Respir. Res. 19 (1) (2018) 243.
[13] R.H. Zhang, et al., Autophagy is involved in the acute lung injury induced by H9N2 influenza virus, Int. Immunopharm. 74 (2019), 105737.
[14] R. Froquet, et al., Control of cellular physiology by TM9 proteins in yeast and Dictyostelium, J. Biol. Chem. 283 (11) (2008) 6764–6772.
[15] B. Pruvot, et al., Comparative analysis of nonaspanin protein sequences and expression studies in zebrafish, Immunogenetics 62 (10) (2010) 681–699.
[16] C.R. Clark, et al., Transposon mutagenesis screen in mice identifies TM9SF2 as a novel colorectal cancer oncogene, Sci. Rep. 8 (1) (2018), 15327.
[17] H.Z. Oo, et al., Identification of novel transmembrane proteins in scirrhous-type gastric cancer by the Escherichia coli ampicillin secretion trap (CAST) method: TM9SF3 participates in tumor invasion and serves as a prognostic factor, Pathobiology 81 (3) (2014) 138–148.
[18] L. Shen, et al., miR-1193 suppresses the proliferation and invasion of human T-cell leukemia cells through directly targeting the transmembrane 9 superfamily 3 (TM9SF3), Oncol. Res. 25 (9) (2017) 1643–1651.
[19] R. Paolillo, et al., Human TM9SF4 is a new gene down-regulated by hypoxia and involved in cell adhesion of leukemic cells, PLoS One 10 (5) (2015) e0126968.
[20] P. He, et al., High-throughput functional screening for autophagy-related genes and identification of TM9SF1 as an autophagosome-inducing gene, Autophagy 5 (1) (2009) 52–60.
[21] L. Sun, et al., TM9SF4 is a novel factor promoting autophagic flux under amino acid starvation, Cell Death Differ. 25 (2) (2018) 368–379.
[22] K. Fan, et al., Lipopolysaccharide-induced dephosphorylation of AMPK-activated protein kinase potentiates inflammatory injury via repression of ULK1-dependent autophagy, Front. Immunol. 9 (2018) 1464.
[23] K.J. Livak, T.D. Schmittgen, Analysis of relative gene expression data using real-time quantitative PCR and the 2(-Delta Delta C(T)) Method, Methods 25 (4) (2001) 402–408.
[24] J. Xiao, et al., Recombinant human PDCD5 (rhPDCD5) protein is protective in a mouse model of multiple sclerosis, J. Neuroinflammation 12 (1) (2015) 117.
[25] K. Wang, et al., Protective features of autophagy in pulmonary infection and inflammatory diseases, Cells 8 (2) (2019).
[26] H. Yang, et al., SIGMAR1/Sigma-1 receptor ablation impairs autophagosome clearance, Autophagy 15 (9) (2019) 1539–1557.
[27] L. Guo, et al., Autophagy inhibition protects from alveolar barrier dysfunction in LPS-induced ALI mice by targeting alveolar epithelial cells, Respir. Physiol. Neurobiol. 283 (2021), 103532.
[28] R. Ren, et al., Verdiperstat attenuates acute lung injury by modulating MPO/mu-calpain/beta-catenin signaling, Eur. J. Pharmacol. 924 (2022), 174940.
[29] W. Li, et al., Nobiletin-ameliorated lipopolysaccharide-induced inflammation in acute lung injury by suppression of NF-kappaB pathway in vivo and vitro, Inflammation 41 (3) (2018) 996–1007.
[30] J. Chluba-de Tapia, et al., Cloning of a human multispanning membrane protein cDNA: evidence for a new protein family, Gene 197 (1-2) (1997) 195–204.
[31] G. Pehote, N. Vij, Autophagy augmentation to alleviate immune response dysfunction, and resolve respiratory and COVID-19 exacerbations, Cells 9 (9) (2020).
[32] Z. Zhang, et al., Genipin protects rats against lipopolysaccharide-induced acute lung injury by reinforcing autophagy, Int. Immunopharm. 72 (2019) 21–30.
[33] S.A. Slavin, et al., Autophagy inhibitor 3-methyladenine protects against endothelial cell barrier dysfunction in acute lung injury, Am. J. Physiol. Lung Cell Mol. Physiol. 314 (3) (2018) L388–L396.
[34] R. Hu, et al., Complement C5a exacerbates acute lung injury induced through autophagy-mediated alveolar macrophage apoptosis, Cell Death Dis. 5 (2014) e1330.
[35] M. Shadab, et al., Autophagy protein ATG7 is a critical regulator of endothelial cell inflammation and permeability, Sci. Rep. 10 (1) (2020), 13708.
[36] W. Dong, et al., RAB26-dependent autophagy protects adherens junctional integrity in acute lung injury, Autophagy 14 (10) (2018) 1677–1692.
[37] Y. Wang, et al., Hydrogen-rich saline ameliorated LPS-induced acute lung injury via autophagy inhibition through the ROS/AMPK/mTOR pathway in mice, Exp. Biol. Med. 244 (9) (2019) 721–727.